Transient-current study of field-assisted emission from shallow levels in silicon

E. Rosencher, V. Mosser, and G. Vincent*
Centre National d'Etudes des Télécommunications—Centre Norbert Segard
Boîte Postale 98, F-38243 Meylan, France
(Received 14 March 1983; revised manuscript received 29 August 1983)

Transient currents due to the emission of carriers trapped on shallow doping levels are investigated in silicon junctions at low temperature. The current-vs-time curves present a peak which can be explained in terms of electric field activation. Simultaneous bulk resistivity measurements allow determination of a temperature range where the transient currents can be properly analyzed, i.e., between 20—25 K. The detrapping kinetics are then analyzed mathematically and the different possible electric field activation mechanisms reviewed: shallow-impurity impact ionization, Frenkel-Poole effect, tunneling, and phonon-assisted tunneling. Three-dimensional calculations are performed for these last two effects and tractable expressions are derived. In Si:P junctions, fairly good agreement between the theoretical model and experimental data is obtained for Frenkel-Poole effect only. In Si:B junctions, an electric-field-dependent peak is observed for ionization transient currents, but it is too broad to be fitted. This is shown to be due to the very high resistivity of our p-type samples in the temperature range investigated. Finally, the value obtained for the electron-capture cross section on phosphorous is discussed.

I. INTRODUCTION

In silicon, the usual donor and acceptor impurities such as phosphorus or boron introduce shallow energy levels, the so-called hydrogenic states, doping the semiconductor to the desired type and density of free carriers. Indeed, at room temperature, the lattice thermal energy is high enough to ionize these levels, providing free carriers. If a reverse potential is applied to a rectifying contact (Schottky diode, p-n junction,...), the free carriers are instantaneously swept away by the surface electric field, resulting in a depletion or space-charge layer. For nondegenerate concentrations of doping impurities at sufficiently low temperatures, carrier "freezeout" occurs, i.e., the density of thermally generated carriers vanishes. Between 20 and 30 K, some free carriers remain available in the silicon bulk, but the emission time constant of these carriers trapped on the doping levels is in the microsecond-millisecond range. Consequently, any increase in the reverse potential applied to a junction will be followed by a slow emission of the carriers from the impurity states in the space-charge region, until the depletion region relaxes into its steady state, i.e., impurities fully ionized.

Only recently have studies of depletion-layer formation in silicon junctions at low temperature been reported in the literature.[1–5]. It has been observed that the detrapping current is not monotonic in time but presents a peak in both n- and p-type Si junctions.[5] Considering the effect of the electric field in the diode on emission kinetics, it has been suggested that this effect may be due either to tunneling effect at very low temperature[1] or to Frenkel-Poole effect at intermediate temperatures.[1–5]

In this paper, we report a detailed experimental and theoretical investigation of the ionization transient currents (ITC) brought about in Si p-n junctions by the ionization of the shallow levels in the space-charge layer at low temperature. It will be shown that, taking the appropriate experimental precautions, the ITC in silicon can be accurately described using a model based on field-enhanced thermal emission. In the temperature range investigated (20—25 K), the Frenkel-Poole effect is shown to fit all our experimental data, contrary to pure or phonon-assisted tunneling. Moreover, the very good agreement between the theoretical model and the experimental data rules out the presence of shallow impurity impact ionization during the ITC, even though electric fields far larger than the critical field do build up in the frozen-out junction during the transient process. This result is explained in terms of the impact ionization mean free path being larger than the width of the depletion layer during the emission transient.

In Sec. II, after description of the experimental technique and device preparation, the experimental results are given. The theoretical analysis is presented in Sec. III: In the case of a uniformly doped junction, the ITC in the diode is shown to be the solution to a set of first-order partial differential equations with one-sided boundary conditions. These equations can be solved numerically without any serious computational problems. The different electric field effects are reviewed and their efficiencies are discussed. The experimental data are compared with the theoretical model in Sec. IV. They are fitted for different sets of temperature and bias conditions. The role of compensation, particularly through its effect on bulk resistivity, is discussed. Finally, the validity of the model, for different ranges of temperature and electric field, is briefly analyzed.

II. DEVICE PREPARATION AND EXPERIMENTS

Experimental devices are fabricated on ⟨100⟩ 3-in Si wafers of the thickness $L=380$ μm, provided by

SILTRONIX. The n-type samples (series N) are 1.3—2.6 Ω cm phosphorus-doped (Si:P), introducing a E_c-44-meV level and the p-type samples (series P) are 1—3 Ω cm boron-doped (Si:B), introducing a E_v+45-meV level.[6] Prior to device preparation, the backside faces are degenerated and damaged in order to yield a good backside Ohmic contact. Using standard planar technology, p^+-n (respectively, n^+-p) junctions are diffused at 1000 °C for 1 h with nominal areas of 60×160 μm (respectively, 310×310 μm). The doping gradient is thus expected to extend over less than 0.6 μm. In order to study the bulk resistivity, neighboring Ohmic contact n^+-n (respectively, p^+-p) of the same geometry was previously diffused. The junction areas are made small as doping striations in the wafers might widen the transient currents observed.

The samples are fixed in a brass flat pack and cooled in a circulating helium cryostat (CRCS Air Liquide). The temperature is stabilized within a few tens of mK and the absolute temperature measured within $\pm$ 100 mK by means of a calibrated platinum resistor. This resistor is placed inside the copper cold head near its extremity and comes within 1 mm of the sample. In order to check against any temperature differences between the sample and the resistor, a calibrated cryogenic linear temperature sensor, (CLTS) was put inside a similar flat pack in place of the sample. The temperatures measured using both the platinum resistor and the CLTS sensor proved to be identical within experimental errors. Finally, during our ITC experiments, typical transient currents are in the 1-μA range on 1-MΩ bulk resistance; therefore, heating of the sample during an ITC is negligible.

At the investigated temperature T, some free carriers remain available in the silicon bulk, so that the semiconductor has not turned into an insulator. This is checked by measuring the bulk resistance in the n^+-n-n^+ (p^+-p-p^+) Ohmic contacts. The diode is forward biased long enough for the carrier flow to fill the impurity states. The applied potential is, however, kept sufficiently low to avoid shallow-level impact ionization. Consequently, at time $t=0^-$, the shallow levels in the junction are in thermal equilibrium with the bulk [Fig. 1(a)]. At time $t=0^+$, the diode is reverse biased. The free carriers in the junction are instantaneously swept away by the electric field. Since most of the doping impurities have been neutralized, the space-charge layer which builds up at the semiconductor surface extends deeply into the bulk. Then the electrons trapped in the space-charge region are thermally emitted [Fig. 1(b)] and swept away by the electric field, resulting in an ionization transient current. This current ceases when a steady state in the emission-recombination mechanisms is reached [Fig. 1(c)].

The transient currents are detected on a charge resistance, amplified by a low-noise preamplifier, and restored by a boxcar averager with a duty cycle of 1%. At each temperature, the following experimental precautions are taken:

(i) The filling pulse duration and bias are enhanced until the ITC becomes stationary.

(ii) The $I(V)$ curves of the diodes are drawn in order to determine the barrier height V_B. A value of 1.1 V is systematically found, and corresponds approximately to the Si gap.

(iii) The bulk resistance $R_b(T)$ is measured through the n^+-n-n^+ (or p^+-p-p^+) Ohmic contacts by means of a 100-mV applied dc bias, i.e., a voltage low enough to avoid any heating of the substrate. Moreover, the $I(V)$ characteristics are checked for linearity up to the critical field where shallow impurity impact ionization occurs, so that the contact can be considered as effectively Ohmic. Since the diodes and the Ohmic contacts have the same geometry, $R_b(T)$ is the largest bulk resistance in series with the diode during the ITC. If $i_{max}R_b(T)$ is not reasonably small compared to the applied potential V_a, most of the potential drop occurs in the semiconductor bulk and the ITC data analysis is not straightforward. Indeed, the bulk resistance changes dramatically during shrinkage of the depletion layer.

Figure 2 shows the curves $\log(R_b)$ vs $1/T$ for samples of both types ($N1$ and $P1$), the ITC of which will be investigated in what is to follow. These curves do not exhibit the two straight sections characteristic of very low compensation.[7] Note that the slope of the curves $\log(R_bT^{3/2})$ vs $1/T$ yields the activation energy of the "freezeout" effect. One finds 44 meV for the n-type sam-

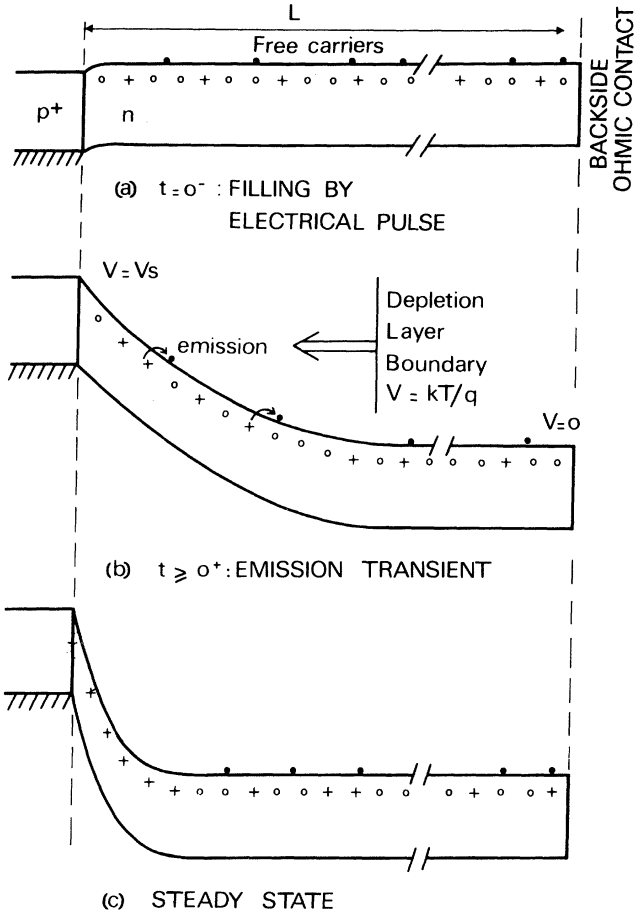

FIG. 1. Energy-band diagrams of a p^+-n junction for different conditions: (a) during the electrical filling pulse, (b) during the doping impurity emission transient, and (c) at steady state.

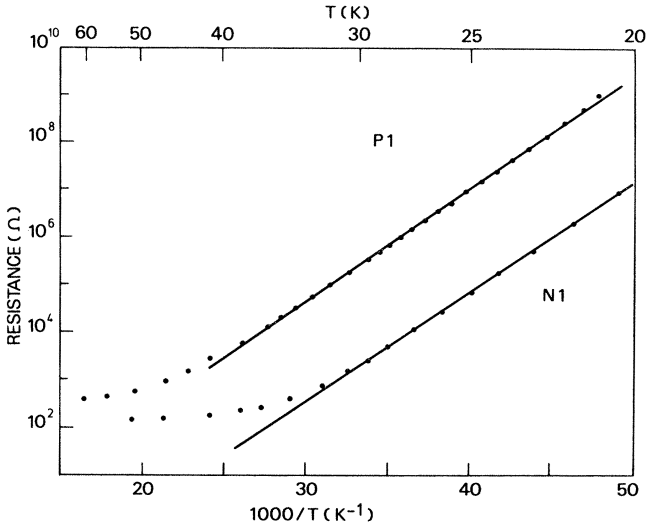

FIG. 2. Semilog plots of bulk resistivity vs temperature in a n-type sample ($N1$) and in a p-type sample ($P1$).

ple and 45 meV in the p-type sample which are the familiar binding energies of the doping impurities.

Typical ionization transient current-versus-time curves in the n-type sample ($N1$) are presented (i) at three different temperatures for the same applied bias in Fig. 3, and (ii) for three different biases at a constant temperature in Fig. 4. A large current overshoot is observed in the current-versus-time curves. The detrapping kinetics are obviously a function of both temperature and electric field in the junction, strongly suggesting the presence of electric-field-assisted thermal emission of trapped carriers from the doping levels. The same effect is also observed in the p-type sample ($P1$) as a function of temperature (Fig. 5) and applied bias (Fig. 6).

III. THEORETICAL MODEL

A. Kinetic equations

In order to account for our experimental ITC's, we have worked out a theoretical model based on an electric-field-assisted emission mechanism of trapped carriers.

Let us first make the following working assumptions.

(i) Charge transport in the space-charge layer is considered as instantaneous, i.e., any charge emitted is immediately collected at the boundary of the depletion layer. Indeed, even in the worst case of a completely depleted 380-μm-thick Si sample, the maximum initial electric fields are typically in the 10^2 V/cm range, leading to transit times shorter than 10 ns.[8] The ITC's are observed over a time scale which is long in comparison to this transit time.

(ii) Shallow impurity impact ionization by the carriers emitted in the space-charge layer is neglected. A detailed discussion is given in Appendix B.

Assuming the above, the carrier flow in the junction is governed by (i) the charge-conservation equations, (ii) Poisson's law, and (iii) the equation describing the emission-recombination mechanism in the diode. The

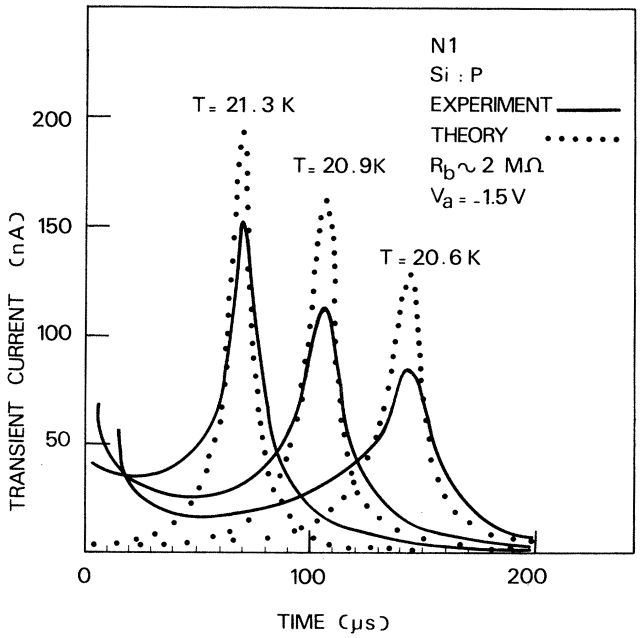

FIG. 3. Ionization transient currents in Si:P p^+-n diode at three different temperatures. The doping impurity concentration is 3×10^{15} cm^{-3}, the junction area 7.5×10^{-5} cm^2. The solid lines refer to the experimental data while the dotted lines are the best fits obtained with the theoretical model. The capture cross section is deduced to be 1.3×10^{-13} cm^2.

equations are written for a one-dimensional n-type junction.

The charge distribution $\rho(x,t)$ in the semiconductor is given by

$$\rho(x,t)=q\{N_D^+(x,t)-[N_A+n(x,t)]\}\ , \tag{1}$$

where $N_D^+(x,t)$ is the concentration of ionized donors and N_A the compensating acceptor concentration. It is as-

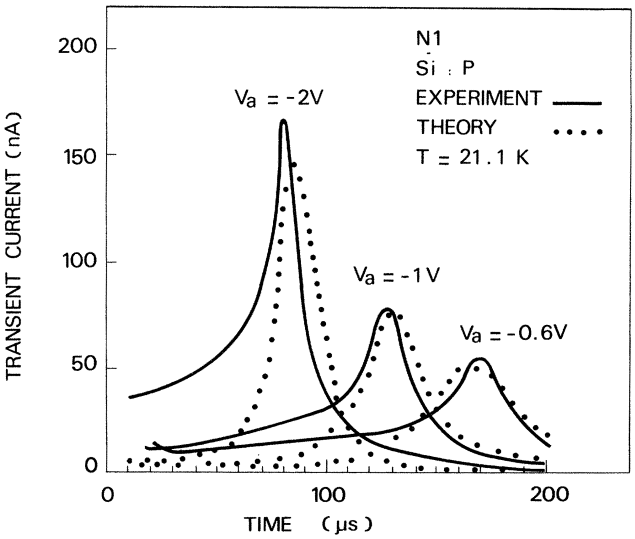

FIG. 4. Ionization transient currents in Si:P p^+-n diode for three applied voltages at 21.1 K. Other sample characteristics are those of Fig. 3.

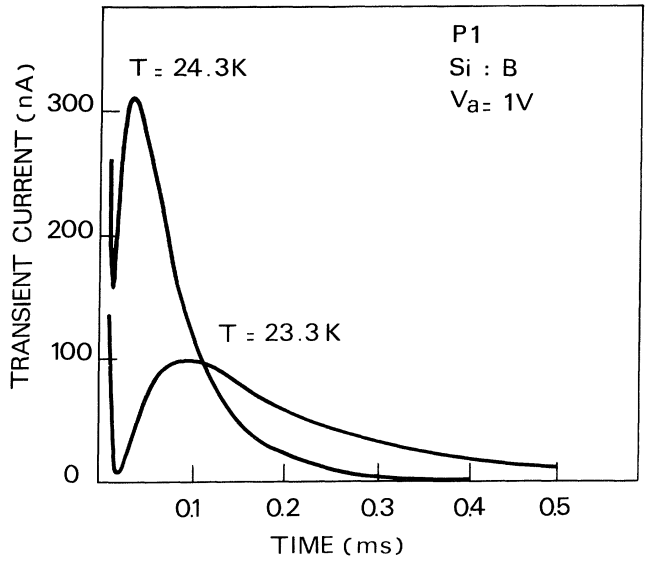

FIG. 5. Large overshoots in ionization transient currents in Si:B n^+-p diode at 23.3 and 24.3 K.

sumed that the emitted carriers are instantaneously in thermal equilibrium with the semiconductor electron gas so that the concentration of free carriers $n(x,t)$ is given by Boltzmann statistics:

$$n(x,t)=n_0 \exp\left[-\frac{(-q)V(x,t)}{kT}\right], \tag{2}$$

where $V(x,t)$ is the potential in the junction and the concentration of bulk free carriers n_0 is given by Fermi-Dirac statistics, taking into account the compensation.[7]

The electric field distribution $F(x,t)$ is governed by Poisson's law:

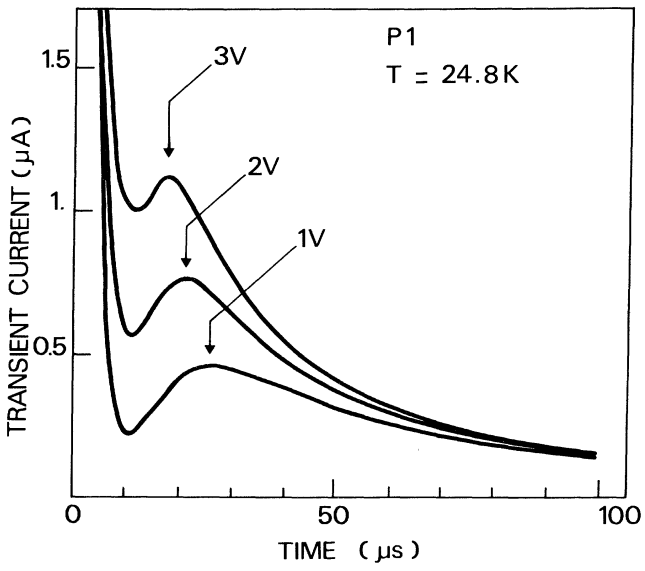

FIG. 6. Ionization transient currents in Si:B n^+-p diode for three different applied voltages at 24.8 K.

$$\left[\frac{\partial F(x,t)}{\partial x}\right]_t = -\left[\frac{\partial^2 V(x,t)}{\partial x^2}\right]_t = \frac{\rho(x,t)}{\epsilon_s}, \tag{3}$$

where ϵ_s is the silicon dielectric constant (1.03×10^{-12} F cm^{-1}).

The kinetic equation describing the generation-recombination mechanism in the semiconductor reads

$$\left[\frac{\partial N_D^+(x,t)}{\partial t}\right]_x = A_T[N_D - N_D^+(x,t)] - B_T N_D^+(x,t) n(x,t), \tag{4}$$

where N_D is the bulk donor concentration and A_T and B_T the emission and recombination rates, respectively.

In the following, all concentrations are expressed in a reduced form, i.e., we introduce

$$y(x,t)=N_D^+(x,t)/N_D, \tag{5a}$$

$$y_0=N_D^b/N_D, \tag{5b}$$

$$\xi=N_A/N_D, \tag{5c}$$

where N_D^b is the ionized donor concentration in the bulk, ($N_D^b=n_0+N_A$), $y(x,t)$ is defined as the ionization coefficient, and ξ as the acceptor compensation factor.

The emission rate A_T is a function of the local electric field. The different numerical expressions for A_T relative to the different electric field effects will be given in Sec. III B. The thermal recombination rate B_T, on the other hand, is assumed not to be affected by the electric field. In any case, in the high-field region of the junction, the recombination term $B_T N_D^+(x,t)n(x,t)$ is negligible, since, according to Boltzmann statistics, $n(x,t)$ is very low. Nevertheless, the presence of this recombination term in Eq. (4) allows one to get rid of the abrupt boundary approximation which is very difficult to handle numerically in our specific problem.

Detailed balance applied under the zero-field conditions then leads to

$$B_T=\frac{e_n}{n_0}\frac{1-y_0}{y_0}, \tag{6}$$

where e_n is the zero-field thermal emission rate (see Sec. III B).

Finally, the ionization transient current collected in the external circuit is given by Gauss's law:

$$i(t)=A\epsilon_s\frac{dF(0,t)}{dt}, \tag{7}$$

where A is the area of the junction.

Equations (3) and (4) constitute a system of second-order partial differential equations having two-sided boundary conditions:

$$y(x,0)=y_0 \quad \text{for } 0<x<L, \tag{8a}$$

$$F(L,t)=0, \tag{8b}$$

$$V(L,t)=0, \tag{8c}$$

$$V(0,t)=V_s, \tag{8d}$$

where V_s is the total barrier height taking into account the built-in barrier height V_B and the applied bias V_a: $V_s = V_B + V_a$.

In the event of high bulk resistance R_b, which has to be expected in silicon at cryogenic temperatures, the boundary conditions (8b)—(8d) must be replaced by

$$F(W,t)=0\ , \tag{8e}$$

$$V(W,t)=kT/(-q)\ , \tag{8f}$$

$$V(0,t)=V_s-R_b i(t)\ . \tag{8g}$$

In fact, condition (8e) is an approximation, since the electric field between the boundary of the depletion layer and the backside contact is not equal to zero. However, except at the very beginning of the detrapping transient, the field near the depletion-layer boundary is small in comparison to the mean electric field in the junction, as long as the bulk resistivity is not overwhelming.

Solving Eqs. (1)—(4) gives rise to important mathematical difficulties. However, in the case of uniform doping, which is assumed in what follows, a set of first-order partial differential equations having one-sided boundary conditions can be written.

Changing the set of variables (x,t) in (V,t) where V is the potential in the semiconductor, Eqs. (3) and (4) become, respectively,

$$\frac{1}{2}\left[\frac{\partial F^2(V,t)}{\partial V}\right]_t=\frac{(-q)N_D}{\epsilon_s}\{[y(V,t)-\xi]-(y_0-\xi)e^{-(-q)V/kT}\} \tag{9}$$

and

$$\left.\frac{\partial y(V,t)}{\partial t}\right|_V=\left[A_T(F)[1-y(V,t)]-e_n\frac{1-y_0}{y_0}y(V,t)e^{-(-q)V/kT}\right]-F(V,t)\left[\frac{\partial y(V,t)}{\partial V}\right]_t\int_V^{V_s}\frac{\partial}{\partial t}\left[\frac{1}{F(V,t)}\right]dV\ , \tag{10}$$

with the boundary conditions

$$F(0,t)=0\ , \tag{11a}$$

$$y(V,0)=y_0 \quad \text{for } 0<V<V_s\ . \tag{11b}$$

Finally, the relationship between the spatial and potential variables is expressed by

$$x=\int_V^{V_s}\frac{du}{F(u)}\ . \tag{12}$$

The integro-differential equations can be solved by an ordinary step-by-step procedure, without any computational problems.

B. Electric-field-assisted emission

Three kinds of electric field effects compete during emission, depending on electric field and temperature conditions. These are (i) the lowering of the impurity potential barrier or Frenkel-Poole (FP) effect (path 1 in Fig. 7), (ii) direct tunneling (TU) across the barrier (path 2 in Fig. 7), (iii) phonon-assisted tunneling (PAT) (path 3 in Fig. 7). Contrary to some author's assertions,[4] these electric field effects also apply to holes emitted from their charged impurity state.[9] Our observation of electric-field-dependent responses in p-type samples during ITC experiments provides, should it be necessary, supplementary proof of this.

Under our experimental conditions, where the energy level of the ground state is very close to the conduction band, all of the three above-mentioned effects are expected to occur. Although the problem of electric-field-assisted emission has been largely analyzed in the literature, numerical solution of our differential equations requires expressions that are easy to handle. Therefore, we shall present a simple analysis of three-dimensional electric field effects.

When no electric field is present, the phonons in the semiconductor give rise to a thermal emission rate e_n, the classical expression of which is based on the detailed-balance principle:

$$e_n=e_n^0\exp\left[-\frac{E_i}{kT}\right]\ , \tag{13}$$

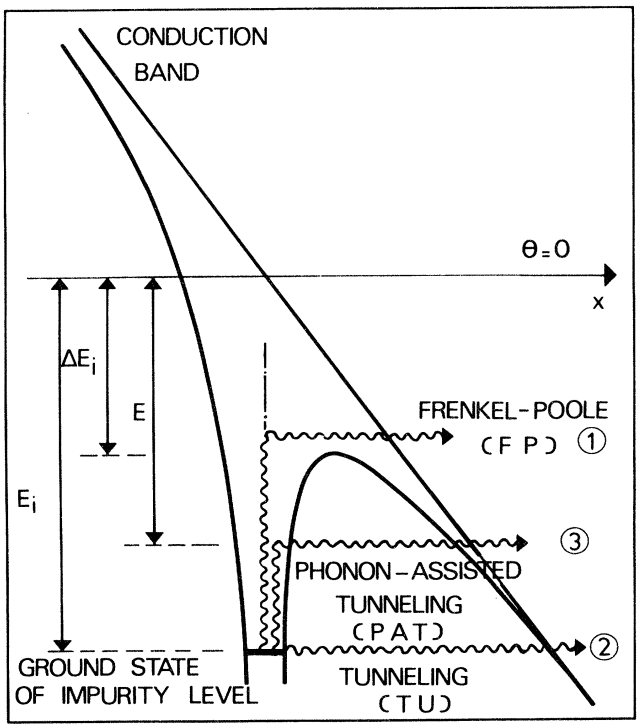

FIG. 7. The three different electric-field-assisted emissions from a Coulombic well.

where E_i is the ionization energy of the doping level. The preexponential term e_n^0 is given by

$$e_n^0=\sigma_n N_c v_{\text{th}}/g \ , \tag{14}$$

where σ_n is the capture cross section, N_c the effective density of states in the conduction band, v_{th} the thermal velocity, and g the degeneracy factor. For a capture cross section σ_n of 1.3×10^{-13} cm^2, (Ref. 5) e_n in silicon is 3×10^{13} $[T/(300\text{ K})]^2$ s^{-1}.

When an electric field F is applied, the potential barrier is lowered by ΔE_i, so that an electron with an energy located between E_i-ΔE_i and E_i is considered to be in the conduction band (see Fig. 7). This is the well-known Frenkel-Poole effect.[10] Assuming that the preexponential factor is not modified by the electric field, the resulting emission rate in the field direction is

$$(e_n^1)_{\text{FP}}=e_n \exp\frac{\Delta E_i}{kT} \ , \tag{15}$$

where the subscript FP specifies the Frenkel-Poole effect and superscript 1 serves as a reminder that this result is valid for a one-dimensional calculation. For a Coulombic well, the lowering of the barrier is given by

$$E_i=q\left[\frac{qF}{\pi\epsilon_s}\right]^{1/2} . \tag{16}$$

The three-dimensional emission rate requires an integration over the whole space, in light of the spatial variation of the lowering. For a Coulombic well, the final emission rate is given by[11]

$$(e_n^3)_{\text{FP}}=e_n\{(1/\gamma^2)[e^\gamma(\gamma-1)+1]+\tfrac{1}{2}\} \ , \tag{17}$$

where $\gamma=\Delta E_i/kT$.

Figure 8 shows the calculated activated thermal emission rate as a function of electric field at $T=24$ K.

As far as the pure tunneling effect is concerned, the emission is a temperature-independent isoenergetic transition from the ground state to the conduction band (Fig. 2). A reasonable approximation for the related three-dimensional emission rate from a Coulombic well is shown to be (see Appendix A)

$$(e_n^3)_{\text{TU}}=\frac{U}{6\hbar}\left[\frac{U}{E_i}\right]^2\exp\left\{-\left[\frac{E_i}{U}\right]^{3/2}\left[1-\left[\frac{\Delta E_i}{E_i}\right]^{5/3}\right]\right\} , \tag{18}$$

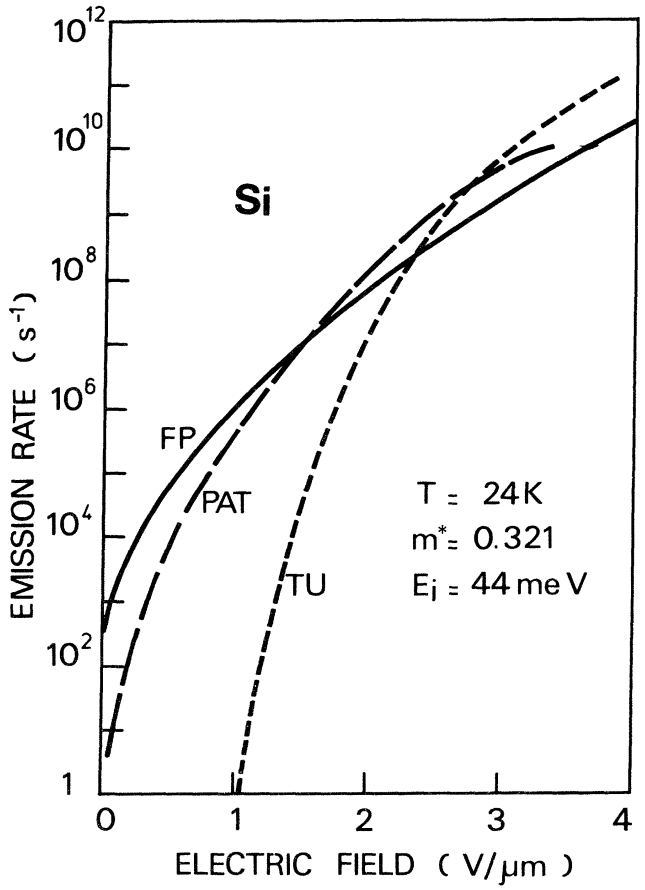

FIG. 8. Emission rates A_T vs electric field for phosphorus donor in silicon. The indication FP refers to the Frenkel-Poole effect, TU to pure tunneling, and PAT to phonon-assisted tunneling. The electron-capture cross section is $\sigma_n=1.3\times10^{-13}$ cm^2.

where $U=[3q\hbar F/(4\sqrt{2m^*})]^{2/3}$ is homogeneous to an energy. The exponential factor represents the transparency of the hyperbolic barrier,[12,13] and the preexponential factor is in the 10^{12}-s^{-1} range in silicon for $F=1$ V/μm. The pure tunneling emission rate is significant only for electric fields larger than 2 V/μm as seen in Fig. 8.

Midway between the Frenkel-Poole and pure-tunnel effects is phonon-assisted tunneling. This is equivalent to the Franz-Keldysh effect for photon absorption in semiconductors under electric field.[12–14] As can be guessed from Fig. 7, calculation of the total phonon-assisted tunnel emission requires a tedious double integration over the $(\Delta E_i, E_i)$ energy range, as well as over the spatial distribution of the electric field. However, it can be shown (see Appendix A) that, if the condition $\Delta E_i/U \gg 1$ is satisfied, and such is the case for the electric fields involved in our experiments, the three-dimensional emission rate reads

$$(e_n^3)_{\text{PAT}}=\frac{e_n}{2}\int_{\Delta E_i}^{E_i}\left[\frac{U}{E}\right]^{3/2}\exp\left\{\frac{E}{kT}-\left[\frac{E}{U}\right]^{3/2}\left[1-\left[\frac{\Delta E_i}{E}\right]^{5/3}\right]\right\}\frac{dE}{kT} . \tag{19}$$

This emission rate is plotted in Fig. 8 for $T=24$ K and the same physical parameters (especially σ_n) as in the Frenkel-Poole effect. In normally doped junctions, the usual electric fields are in the few V/μm range so that the three processes are expected to occur during the ITC.

C. Illustrative numerical results

As an illustrative example, the kinetic equations have been solved for a Si p^+-n diode at $T=24$ K assuming only the Frenkel-Poole effect, with $\sigma_n=1.3\times10^{-13}$ cm^2. The doping concentration is 3×10^{15} cm^{-3} with an impurity level at 44 meV, the acceptor compensation factor zero and the total surface potential 1 V. Figures 9(a) and 9(b) show the ionization coefficient $y(x,t)$ and the electric-field distribution $F(x,t)$, respectively, at different times. The resulting transient current is shown in Fig. 9(c). The large current overshoot can be explained as follows.

At the beginning of the detrapping transient, the equilibrium free-carrier concentration n_0 being low $(10^{-5}N_D-10^{-3}N_D)$, the corresponding depletion layer is wide (>100 μm). The field at the semiconductor surface is low and the carriers are emitted from their doping level

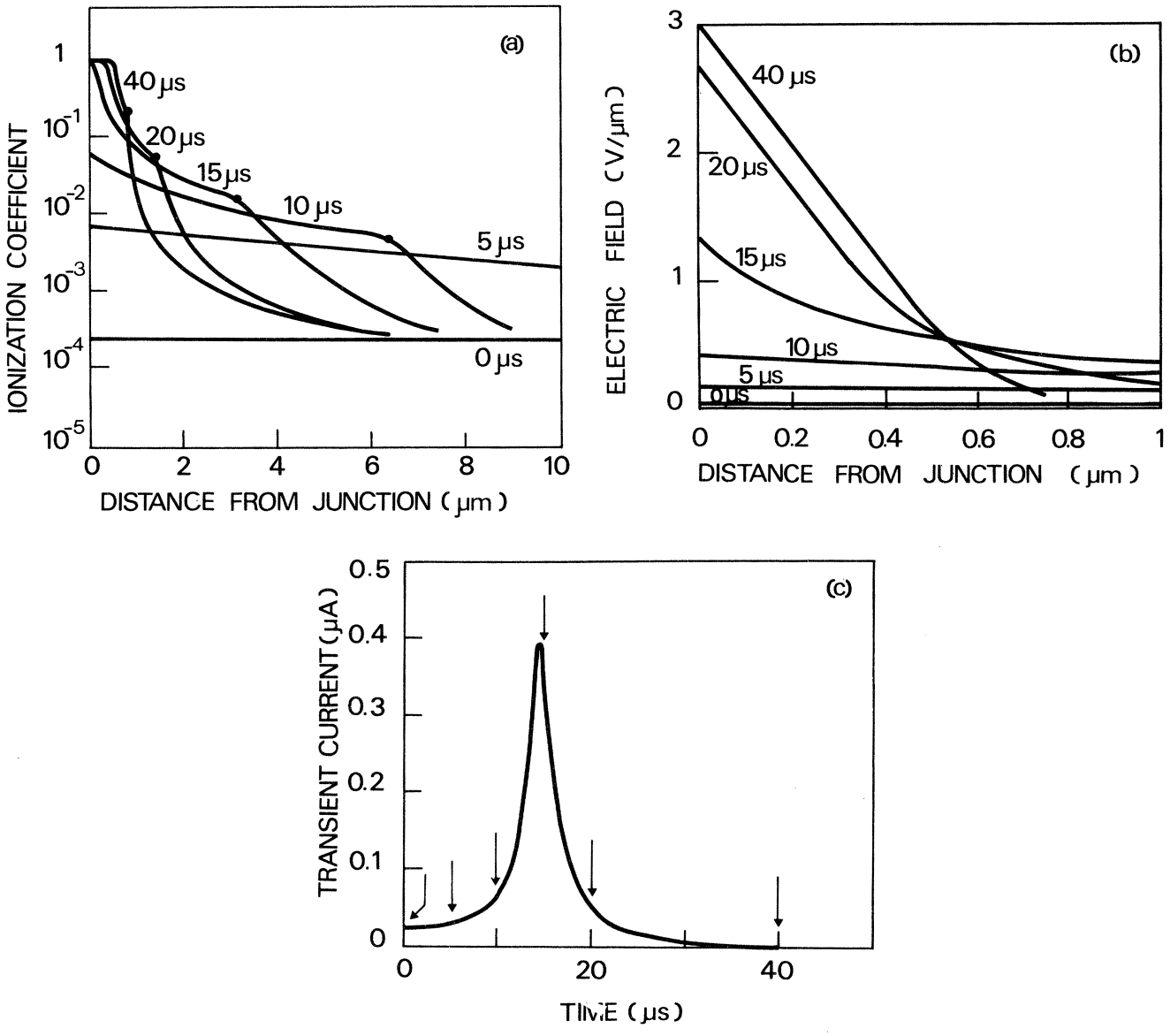

FIG. 9. Calculated transient behavior of a p^+-n Si:P diode at $T=24$ K. The donor concentration is 3×10^{15} cm^{-3}, the junction area is 7.5×10^{-5} cm^2, and the electron-capture cross section is 1.3×10^{-13} cm^2. (a) Ionization coefficient distribution vs distance with time as a parameter; the dots indicate the conventional depletion-layer boundary, where $V=kT/q$. (b) Electric field distribution vs distance for the same sampling times as in 9(a). (c) The corresponding ionization transient current-vs-time curve; the sampling times of curves a and b are indicated by arrows.

with the slow thermal emission coefficient e_n. As the impurities become more and more ionized, the space-charge layer shrinks and the field increases near the semiconductor surface. The barrier lowering by Frenkel-Poole effect becomes predominant and the field activation is dramatically enhanced, resulting in the increase in the ITC observed in Fig. 9(c).

Clearly, the initial conditions of the detrapping kinetics are governed by the ionized donor concentration N_D^b [see Eq. (5a)]. But, at cryogenic temperatures, N_D^b is essentially a function of the residual acceptor concentration which is not accurately known. Consequently we have investigated the influence of the compensating factor ξ on the transient currents calculated. Figure 10 shows the results of the simulation for $\xi=0$ and $\xi=3.3\times10^{-3}$ at $T=21.1$ K, with the same device parameters as in Fig. 9. The increase in ξ leads to only a slight displacement of the current peak, leading us to conclude that the influence of ξ on the detrapping kinetics can be neglected. The influence of compensation on the bulk resistance R_b is crucial, however, and will be analyzed in the next section.

IV. ANALYSIS OF RESULTS

A. Comparison between experiment and theory

We have compared our experimental data, obtained as described in Sec. II, with the theoretical model, using the different emission rates A_T corresponding to the different electric field effects.

Figure 3 shows such a comparison for the n-type sample ($N1$) at three different temperatures (for bulk resistance, see Fig. 2). The solid lines represent the experimental curves, while the dots refer to the theoretical model in which the expressions for the Frenkel-Poole effect have been used. It can be seen that the agreement between the two is quite good. The unique fitting parameter is the electron-capture cross section; its best value is found to be $\sigma_n=1.3\times10^{-13}$ cm^2. The fit was not possible assuming a tunnel effect, which is temperature independent, but seemed practicable for phonon-assisted tunneling. However, this latter mechanism did not allow us to fit the bias dependence of the ITC. On the contrary, agreement between the theoretical model based on the Frenkel-Poole effect and experimental ITC's for three different applied biases at $T=21.1$ K was fairly good (see Fig. 4). This strongly suggests that the Frenkel-Poole effect is the dominant electric field mechanism in this temperature and electric field range. The slight discrepancy at the beginning of the transient (e.g., see Fig. 3) may originate from (i) the *high compensation* due to the p^+ dopant diffusion over the first 0.6 μm of the junctions and/or (ii) the higher electric field at the edge of the diode. Both effects may result in an enhancement of the emission rate, short-circuiting the main ITC at the very beginning. Whatever that may be, we have checked that the total charge emitted during the ITC is consistent with the total charge in the depletion region of the devices.

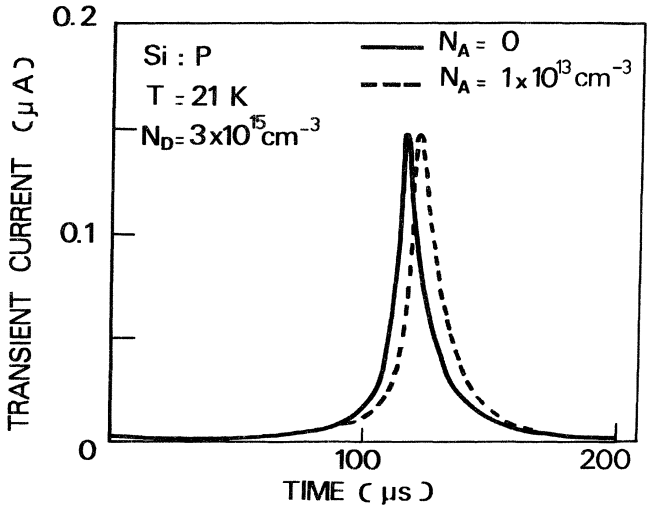

FIG. 10. Calculated influence of the semiconductor compensation on the ionization transient current at 21 K: bulk resistivity is assumed to be zero. Other sample characteristics are those of Fig. 9.

Let us point out that, for n-type material, the product $i_{\max}R_b(T)$ is at most in the few 100-mV range, which is reasonably small compared to the applied voltages. This is not the case in the Si:B junctions, the ITC's of which could not be fitted. The current-versus-time curves in Figs. 5 and 6 are indeed too broad. In these last samples, bulk resistivity is so high that most of the potential drop occurs in the silicon bulk. Below $T=22$ K, no current overshoots are observed in our n^+-p diodes. This is consistent with Tewksbury's results. This author did not observe electric-field-dependent features in current-versus-time characteristics in metal-oxide-semiconductor (MOS) field-effect transistors. Indeed, most of his experiments were performed between 12 and 21 K.[4]

The huge variations in semiconductor bulk resistivity from one sample to another at the same temperature originate from different compensation. From the curve $\log(R_bT^{3/2})$ vs $1/T$, and using mobility data already published in the literature,[15] one can estimate the compensating factors.[7] One finds approximately $\xi=5\times10^{-3}$ for our n-type samples and 3×10^{-2} for the p-type ones. These values are in reasonable agreement with the supplier's specifications. The compensation factor higher in our p-type samples than in the n-type was found to be systematic.

B. Discussion

Our investigation of the ionization transient currents—both experimental and theoretical—has been deliberately limited to a temperature range where the semiconductor is not a perfect insulator and to transient processes in the microsecond-millisecond range. We have shown that, under these conditions, the ITC can be accurately described by a model using only the Frenkel-Poole effect.

At higher temperatures (i.e., 77 K), the Frenkel-Poole effect is even more dominant over the other effects. The presence of this field-assisted emission has important technological implications. For cryogenic devices operat-

ing at the temperature of liquid nitrogen, the emission time constant is not in the nanosecond range as might be predicted when solely taking into account the thermal mechanism. This would have drastic consequences on the time response of devices, but owing to field activation, the emission time constant remains in the picosecond range. Moreover, at these temperatures, the emission of trapped carriers is no longer a device limitation. Indeed, the time constant due to the charging of the device capacitance C through the bulk resistance becomes preponderant, i.e., $R_b C \gg e_n^{-1}$.

At lower temperatures ($T < 20$ K), the respective yields from the different field-emission mechanisms change. Between 10 and 15 K, phonon-assisted tunneling should become predominant over most of the electric-field range (0.5—4 V/μm). At even lower temperature ($T < 10$ K), pure tunneling is the only effective mechanism: Emission can be observed only for a high electric field ($F > 2$ V/μm). Since, for these temperatures, the depletion layer expands over the whole sample thickness at time $t = 0^+$, this effect can be obtained only in thin bulk devices, as observed by Banavar *et al.*[1] in p-i-n diodes, for instance.

Another consequence of such low temperatures is that the semiconductor goes into an insulating state ($\rho > 10^{10}$ Ω cm below 14 K in sample $N1$). Transient currents can no longer be described using our model. The formalism of charge emission and transport in insulators must then be used, involving considerable deviation from Ohm's law.[16,17] This explains the difficulty of other authors to account for their experimental results: Their investigated temperature range was indeed too low (10—20 K).[3,4]

As far as the electron-capture cross section on phosphorus is concerned, the value $\sigma_n = 1.3 \times 10^{-13}$ cm^2 obtained is more than 1 order of magnitude lower than the values determined by Norton *et al.* through recombination time measurements, i.e., $\sigma_n \cong 4 \times 10^{-12}$ cm^2 (Ref. 18) or by Brown *et al.* through double injection experiments, i.e., $\sigma_n \cong 7 \times 10^{-12}$ cm^2 at 4 K for $F \cong 0.1$ V/μm.[19] These giant capture cross sections are accounted for by a cascade mechanism:[20] The electron is captured by the impurity on an excited state of large radius; then a one-phonon transition to the ground state occurs. However, in our experiments, these excited states have very short lifetimes, due to the high value of the electric fields involved. In the framework of the quasistationary perturbation theory,[21] the lifetime of the level $E_i = 11$ meV which corresponds to the principal quantum number $n = 2$ of phosphorus levels is given by the tunneling probability: It decreases from a few seconds for $F = 0.1$ V/μm down to the picosecond range for $F = 0.25$ V/μm. Consequently, these excited states can be considered as instantaneously destroyed by the electric field. Only the ground state is involved in the capture mechanism, which yields a capture cross section in agreement with the ground-state Bohr radius.[22]

V. CONCLUSION

We have investigated the ionization transient currents brought about in silicon junctions by the emission of trapped carriers from doping levels. The study has been limited to temperature range in which the semiconductor is not highly resistive so that the potential drop in the substrate during the ITC will not be overwhelming. This calls for simultaneous resistivity measurements, which have been performed in this study. For low-enough bulk resistivity, the ITC's have been shown to be accurately described by a model based on the Frenkel-Poole effect. This fitting was not found possible using our expressions for the other electric field effects (tunnel, phonon-assisted tunnel). In addition the very good agreement between the theoretical model and experimental data rules out the presence of shallow impurity impact ionization, although electric fields far larger than the critical field build up in the frozen-out junctions during an ITC. In fact, under our experimental conditions, the probability for an emitted carrier to yield impact ionization throughout the whole depleted layer is predicted to be small compared to one. Moreover, compensation is proved to play a dominant role since it dramatically enhances bulk resistivity without significantly changing the formation kinetics of the depletion layer. Indeed, owing to high compensation in our Si:B samples, transient currents in n^+-p diodes could not be fitted although large electric-field-dependent peaks were also observed. We believe that it is for this same reason that Tewksbury[2] did not observe any electric-field-dependent features in the reported current-versus-time characteristics. This author's measurements were indeed performed at much lower temperature than ours. Finally, the electron-capture cross section on phosphorus is found to be $\sigma_n = 1.3 \times 10^{-13}$ cm^2 which is the same value as that given by Saks *et al.*[3] The difference between our value and larger ones obtained by other authors is explained by the instantaneous destruction of excited impurity states by the intense electric fields involved in our measurements, decreasing the capture probability of carriers on large radius orbitals.

ACKNOWLEDGMENTS

The authors are deeply indebted to Professor J. C. Pfister for his many critical comments and valuable advice. They also wish to thank Dr. D. Bois, Professor J. Bok, Professor D. Calecki, and Dr. J. F. Palmier for fruitful discussions. Thanks are also due to J. Dargent for a critical reading of the manuscript.

APPENDIX A: THREE-DIMENSIONAL ELECTRIC FIELD EFFECTS

In this appendix, we derive the emission rate for three-dimensional tunneling and phonon-assisted tunneling effect.

1. Tunneling effect for a Dirac well

Pure tunneling for ionization of impurity states in semiconductors has been calculated by Korol[23] for a one-dimensional Dirac well (DW). We rewrite this author's expression in the form

$$(e_n^1)_{TU}=\left[\frac{U}{3\hbar}\right]\left[\frac{U}{E_i}\right]^{1/2}\exp\left[-\left[\frac{E_i}{U}\right]^{3/2}\right], \quad \text{(A1)}$$

introducing the characteristic energy U,

$$U=\left[\frac{3q\hbar F}{4\sqrt{2m^*}}\right]^{2/3}. \quad \text{(A2)}$$

As pointed out by Martin *et al.*,[24] it is a dubious practice to use the effective-mass approximation for localized states, however difficult this may be to avoid. At any rate, since we are dealing with shallow levels, the effective-mass approximation is certainly not too bad an approach.

For comparison purposes, the different characteristic energies, barrier lowering ΔE_i and U are plotted in Fig. 11 as a function of the electric field. In silicon, for $F=1$ V/μm, a typical preexponential value in (A1) is 10^{12} s^{-1}.

Let us now estimate the three-dimensional tunnel emission rate for a Dirac well. Assuming no tunnel emission in the direction opposite to the electric field, the three-dimensional tunnel emission rate reads, in the Eulerian referential where $\theta=0$ in the electric field direction:

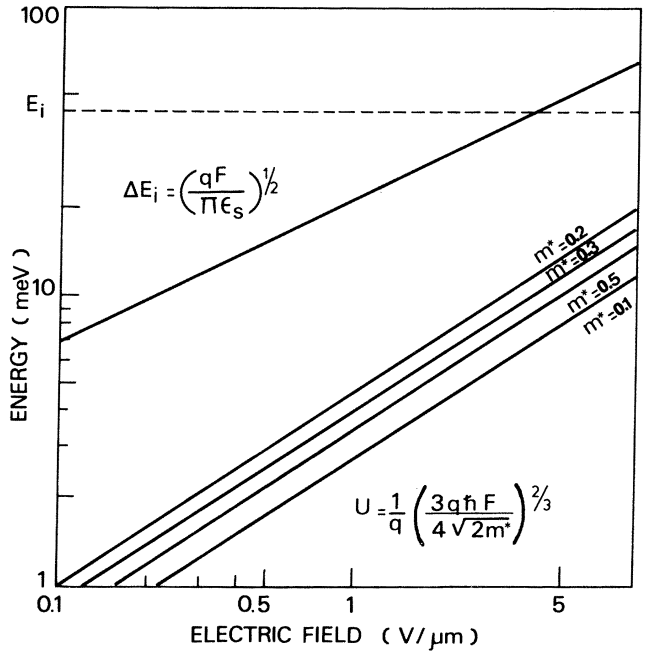

FIG. 11. Plots of different characteristic energies as a function of electric field F: ΔE_i is the barrier lowering via the Frenkel-Poole effect and U is a characteristic energy for phonon-assisted tunneling and pure tunneling calculations. For comparative purposes, the impurity energy level E_i for a phosphorus donor is also indicated.

$$(e_n^3)_{TU}=\frac{1}{4\pi}\int_0^{2\pi}d\phi\int_0^{\pi/2}\left[\frac{U}{3\hbar}\right]\left[\frac{U}{E_i}\right]^{1/2}\cos\theta\exp-\left[\left[\frac{E_i}{U}\right]^{3/2}\frac{1}{\cos\theta}\right]\sin\theta\,d\theta\,. \quad \text{(A3)}$$

In our specific case where $E_i/U\gg 1$ (see Fig. 11), expression (A3) can be approximated by the following expression:

$$(e_n^3)_{TU}=\frac{U}{6\hbar}\left[\frac{U}{E_i}\right]^2\exp\left[-\left[\frac{E_i}{U}\right]^{3/2}\right]. \quad \text{(A4)}$$

2. Tunneling effect for a Coulombic well

The problem of the three-dimensional field ionization from a Coulombic well is a classical one (see for instance S. Chaudhuri *et al.*[25]). However, the available expressions for three-dimensional tunnel emission rate are somewhat complicated and the numerical calculation for our model needs tractable expressions. Therefore we propose in the following a heuristic approach of this effect.

In expression (A1), the exponential factor is exactly the transparency of a triangular barrier of height E_i and base E_i/qF, using the WKB approximation. It seems therefore legitimate to estimate the tunnel emission rate for the Coulombic well by an equivalent expression, but with an exponential term corresponding to the transparency of the hyperbolic barrier defined by the Coulombic potential and the electric field. Using this formulation, Hill gives an approximated analytical expression of $(e_n 1)_{TU}$ for a Coulombic well[26] but the formula is rather complicated.

We have shown[12] that the WKB transparency for an hyperbolic well can be approximated by the simple expression:

$$T_{WKB}=\exp\left\{-\left[\frac{E_i}{U}\right]^{3/2}\left[1-\left[\frac{\Delta E_i}{E_i}\right]^{5/3}\right]\right\}. \quad \text{(A5)}$$

In the frame of this approach, the tunnel emission across a three-dimensional Coulombic well is then obtained by replacing the transparency of the triangular barrier in Eq. (A3) by the transparency of the hyperbolic barrier (A5), which yields

$$(e_n^3)_{TU}=\frac{U}{6\hbar}\left[\frac{U}{E_i}\right]^2\exp\left\{-\left[\frac{E_i}{U}\right]^{3/2}\left[1-\left[\frac{\Delta E_i}{E_i}\right]^{5/3}\right]\right\}. \quad \text{(A6)}$$

3. Phonon-assisted tunneling

Instead of performing an isoenergetic transition from the impurity state to the conduction band, the electron in

the impurity level can be excited by lattice phonons to an energy E, closer to the conduction band, followed by tunneling through the hyperbolic barrier (Fig. 2). The frequency of such a jump is given by

$$\nu = e_n^0 \exp\left[-\frac{E_i - E}{kT}\right] \tag{A7}$$

and the contribution of this transition to the phonon-assisted emission rate is therefore

$$\nu' = e_n^0 \exp\left[-\frac{E_i - E}{kT}\right] \times \exp\left\{-\left[\frac{E}{U}\right]^{3/2}\left[1-\left[\frac{\Delta E_i}{E}\right]^{5/3}\right]\right\}, \tag{A8}$$

where the second exponential term is the transparency of the hyperbolic barrier.

This approach is somewhat different from those found in the literature. Some authors like Lundström and Svensson[27] begin the calculation assuming only isoenergetic transitions from the impurity state to the conduction band and extend their result to temperature-dependent tunneling by multiplying the tunneling probability by an appropriate Fermi distribution. This approach yields the same expression, except for the preexponential term.

A third approach is an *ab initio* complete calculation, taking into account multiphonon processes.[28–30] For a Dirac well, Kudzmauskas finds the same exponential factor which is, indeed, the WKB transparency of the triangular well.

The calculation of the one-dimensional emission rate requires an integration over energy from $E = \Delta E_i$ to $E = E_i$ which yields

$$(e_n^1)_{\mathrm{PAT}} = e_n^0 \exp\left[-\frac{E_i}{kT}\right] \int_{\Delta E_i}^{E_i} \exp\left\{\frac{E}{kT} - \left[\frac{E}{U}\right]^{3/2}\left[1-\left[\frac{\Delta E_i}{E}\right]^{5/3}\right]\right\}\frac{dE}{kT}, \tag{A9}$$

where kT normalizes the integral.[12]

The three-dimensional calculation is tedious. However, if the condition $\Delta E_i / U \gg 1$ is satisfied, the same approximation as the one used for the pure-tunneling three-dimensional calculation can be used and the actual three-dimensional PAT rate is given by

$$(e_n^3)_{\mathrm{PAT}} = \frac{e_n^0}{2} \exp\left[-\frac{E_i}{kT}\right] \int_{\Delta E_i}^{E_i} \left[\frac{U}{E}\right]^{3/2} \exp\left\{\frac{E}{kT} - \left[\frac{E}{U}\right]^{3/2}\left[1-\left[\frac{\Delta E_i}{E}\right]^{5/3}\right]\right\}\frac{dE}{kT}. \tag{A10}$$

APPENDIX B: SHALLOW IMPURITY IMPACT IONIZATION DURING THE DETRAPPING TRANSIENT

Since the ionization energy of shallow impurities is in the 40-meV range, breakdown occurs in Si at cryogenic temperatures for electric fields of a few 100 V/cm.[31,32] This critical value is immediately reached in the space-charge region of the diode at the beginning of the ITC so that impact ionization may be expected to occur during the transport of the emitted carriers through the space-charge layer, as already mentioned in the literature.[1–5]

Instead of performing tedious calculations on transport equations during the ITC we shall determine the probability P for a carrier emitted at the semiconductor surface ($x = 0$) to induce impact ionization in the space-charge layer. For this purpose, we introduce an impact ionization mean free path $\lambda(x)$ which is defined as

$$P_{x,x+dx} = \frac{dx}{\lambda(x)}, \tag{B1}$$

where $P_{x,x+dx}$ denotes the probability of one collision between x and $x + dx$.

If the impact process is Poissonian, which is generally assumed, the mean free path is related to the impact ionization rate A_I through the relation[33]

$$\lambda(x) = \frac{1}{[N_D - N_D^+(x)]\bar{\sigma}_i(\epsilon)}, \tag{B2}$$

where $\bar{\sigma}_i(\epsilon) = A_I(\epsilon)/v_d(\epsilon)$ is the mean impact ionization cross section, and ϵ and v_d the mean carrier energy and drift velocity, respectively. This term is obtained by averaging the microscopic quantity $\sigma_i(\epsilon)$ over the electron distribution function. We have assumed a displaced Maxwellian distribution with an electron temperature T_e. The parameters used for silicon are taken from Ref. 34.

We have used two impact ionization cross-section models: the constant capture cross-section model of Zylbersztejn,[35]

$$\sigma_i(\epsilon)=\begin{cases}0\ , & \epsilon<E_i\\ \sigma_0\ , & \epsilon>E_i\end{cases} \tag{B3}$$

and the hydrogenlike capture cross-section model of Palmier,[36]

$$\sigma_i(\epsilon)=\begin{cases}0\ , & \epsilon<E_i\\ \sigma_0\dfrac{\epsilon-E_i}{E_i}\ , & E_i<\epsilon<2E_i\\ 2\sigma_0\dfrac{E_i}{\epsilon}\ , & \epsilon>2E_i\ ,\end{cases} \tag{B4}$$

where σ_0 is the Bohr section in silicon ($\sigma_0=1.2\times10^{-13}$ cm^2). These models have been shown to compare well with experimental data, yielding calculated values of A_I as a function of electric field slightly higher than the available experimental data.[35–37]

For an electric field of 1000 V/cm and a neutralized donor concentration of 10^{15} cm^{-3}, the impact ionization mean free path is in the 100-μm range. This large value is explained by the ionization energy of the donors in Si, which is larger than the mean intervalley phonon energy. This may also explain the difficulty to obtain an avalanche behavior for shallow impurity impact ionization in Si samples.[38,39]

With these parameters, the probability P can be calculated, for each time, by

$$1-P=\exp\left[-\int_0^W\frac{dx}{\lambda(x)}\right], \tag{B5}$$

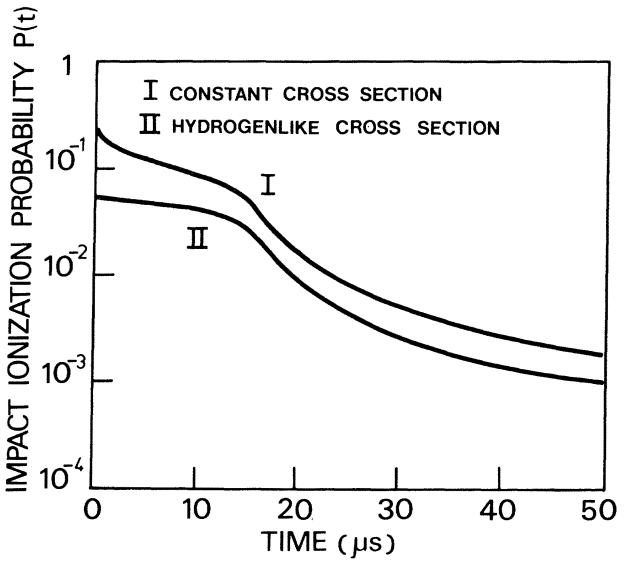

FIG. 12. Probability as a function of time for a carrier emitted at the junction surface to yield shallow impurity impact ionization within the depletion layer. Curves I and II refer to the constant and hydrogenlike cross-section models, respectively. The other parameters are those of Fig. 9.

where W is the depletion-layer boundary. The result of this calculation for the numerical example of Sec. III C is shown in Fig. 12 for both cross-section models. The probability $P(t)$ is indeed small compared to 1 and shallow impurity impact ionization is expected to be negligible during the ITC process.

*Permanent address: Institut National des Sciences Appliqueés, Bâtiment 502, 20 avenue Albert Einstein, F-69621 Villeurbanne, France.

[1]J. R. Banavar, D. D. Coon, and G. E. Derkits, Phys. Rev. Lett. 41, 576 (1978).
[2]J. R. Banavar, D. D. Coon, and G. E. Derkits Jr., Appl. Phys. Lett. 34, 94 (1979).
[3]N. S. Saks and A. Nordbryhn, J. Appl. Phys. 50, 6962 (1979).
[4]S. K. Tewksbury, J. Appl. Phys. 53, 3865 (1982).
[5]E. Rosencher, V. Mosser, and G. Vincent, Solid State Commun. 45, 629 (1983).
[6]F. J. Morin and J. P. Maita, Phys. Rev. 96, 28 (1954).
[7]K. Seeger, *Semiconductor Physics* (Springer, New York, 1973).
[8]H. Lemke and G. O. Muller, Phys. Status Solidi 24, 127 (1967).
[9]A. Chantre, M. Kechouane, and D. Bois, *Defects in Semiconductors,* edited by S. Mahajan and J. W. Corbett (North-Holland, New York, 1982), p. 547.
[10]J. Frenkel, Phys. Rev. 54, 647 (1938).
[11]J. L. Hartke, J. Appl. Phys. 39, 4871 (1968).
[12]G. Vincent, thesis, University of Lyon, France, 1978 (unpublished).
[13]G. Vincent, A. Chantre, and D. Bois, J. Appl. Phys. 50, 5484 (1979).
[14]S. F. Timashev, Fiz. Tverd. Tela 14, 171 (1972) [Sov. Phys.—Solid State 14, 136 (1972)].
[15]P. Norton, T. Braggins, and H. Levinstein, Phys. Rev. B 8, 5632 (1973).
[16]A. Many and G. Rakavy, Phys. Rev. 126, 1980 (1962).
[17]M. A. Lampert and P. Mark, *Current Injection in Solids* (Academic, New York, 1970).
[18]P. Norton, T. Braggins, and H. Levinstein, Phys. Rev. Lett. 30, 488 (1973).
[19]J. M. Brown and A. G. Jordan, J. Appl. Phys. 37, 337 (1966).
[20]M. Lax, Phys. Rev. 119, 1502 (1960).
[21]L. D. Landau and E. M. Lifshitz, *Quantum Mechanics, Non-Relativistic Theory* (Pergamon, New York, 1965).
[22]The Stark shift has been neglected in the discussion. Indeed, such an effect is negligible for applied electric fields less than the classical critical field F_c, in which case carriers must tunnel through an appreciable barrier width ($F_c\cong4.0$ V/μm in Si). See, for instance, S. Chaudhuri, D. D. Coon, and G. E. Derkits, Appl. Phys. Lett. 37, 111 (1980).
[23]E. N. Korol, Fiz. Tverd. Tela 19, 2266 (1977) [Sov. Phys.—Solid State 19, 1327 (1977)].
[24]P. A. Martin, B. G. Streetman, and K. Hess, J. Appl. Phys. 52, 7409 (1981).
[25]S. Chaudhuri, D. D. Coon, G. E. Derkits, and J. R. Banavar, Phys. Rev. 23, 1657 (1981).

[26]R. M. Hill, Philos. Mag. 23, 59 (1971).
[27]I. Lundström and C. Svensson, J. Appl. Phys. 43, 5045 (1972).
[28]S. P. Kudzmauskas, Fiz. Sb. Litow 16, 549 (1976).
[29]D. Pons and S. Makram-Ebeid, J. Phys. (Paris) 40, 1161 (1979).
[30]S. Makram-Ebeid and M. Lannoo, Phys. Rev. B 25, 6406 (1982).
[31]J. Bok, J. C. Sohm, and A. Zylbersztejn, in *Proceedings of the Conference On Semiconductor Physics, Prague, 1960,* edited by K. Zaveta (Publishing House of the Czechoslovak Academy of Sciences, Prague, 1961), p. 138.
[32]M. Asche, H. Kostial, and O. G. Sarbey, Phys. Status Solidi B 91, 521 (1979).
[33]F. Reif, *Fundamentals of Statistical and Thermal Physics* (McGraw-Hill, New York, 1965).
[34]E. Rosencher, Solid State Commun. 38, 1293 (1981).
[35]A. Zylbersztejn, Phys. Rev. 127, 3 (1962).
[36]J. F. Palmier, Phys. Rev. 6, 4557 (1972).
[37]E. Rosencher and J. F. Palmier (unpublished).
[38]A. Zylbersztejn, thesis, University of Paris, France, 1965 (unpublished).
[39]Size effects for shallow impurity impact ionization avalanches have also been reported in Ge sample. See B. M. Vul, E. I. Zavaritzkaya, and J. V. Davydova, Fiz. Tverd. Tela 5, 1107 (1963) [Sov. Phys. Solid State 5 808 (1963)].